NACA

RESEARCH MEMORANDUM

AXIAL-FLOW COMPRESSOR ROTATING-STALL AND ROTOR-BLADE VIBRATION SURVEY

By Howard F. Calvert, Arthur A. Medeiros, and Floyd B. Garrett

Lewis Flight Propulsion Laboratory
Cleveland, Ohio

NATIONAL ADVISORY COMMITTEE
FOR AERONAUTICS

WASHINGTON

May 23, 1955

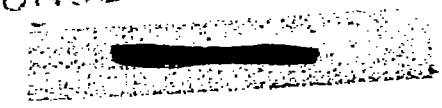

NATIONAL ADVISORY COMMITTEE FOR AERONAUTICS

RESEARCH MEMORANDUM

AXIAL-FLOW COMPRESSOR ROTATING-STALL AND ROTOR-BLADE VIBRATION SURVEY

By Howard F. Calvert, Arthur A. Medeiros, and
Floyd B. Garrett

SUMMARY

A compressor-rotor-blade vibration survey was conducted on a production turbojet engine incorporating a 13-stage axial-flow compressor with a pressure ratio of approximately 7 and having an air flow of 120 pounds per second. Resistance-wire strain gages were used to measure the vibratory stresses in the first three stages and hot-wire anemometers were used to detect rotating stall. A vibratory stress of ±31,200 pounds per square inch excited by a six-zone rotating-stall pattern was measured in the first stage at approximately 5540 rpm. The failure of a fourth-stage aluminum rotor blade concluded the investigation.

INTRODUCTION

Fatigue failures of compressor rotor blades have been a major problem in the development of the axial-flow compressor. The source of many failures has been rotor-blade vibration excited by rotating-stall (refs. 1 and 2). The vibration survey reported in reference 1 was conducted to determine the cause of the first-stage rotor-blade failures occurring in service in a 13-stage production compressor. The source of excitation for the critical vibration was found to be rotating stall. The blades in the first seven stages were fabricated from an aluminum alloy. Aluminum alloy, with its extremely low endurance limit, is very susceptable to fatigue failure due to rotor-blade vibration. This aluminum-bladed compressor was replaced by a design in which the blades in the first three stages were fabricated from a 13-percent-chromium steel. The number of blades in the first stage was reduced by one and in the second stage by two; the airfoil area taper ratio for all three stages was increased.

As a result of these design changes, the investigation reported herein was conducted to determine the rotating-stall and blade-vibration characteristics of the new production compressor. The investigation was conducted in a NACA Lewis static sea-level test stand. The vibratory stresses were measured by the use of resistance-wire strain gages, and

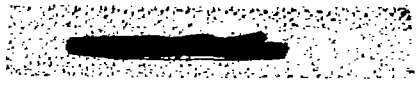

flow fluctuations of rotating stall were detected by the use of constant-current hot-wire anemometers. Steady-state pressures and temperatures were measured at several stations throughout the compressor. The engine was equipped with a variable-area exhaust nozzle to vary the pressure ratio or air flow at a constant speed.

APPARATUS

Turbojet engine. - The investigation was conducted on a turbojet engine incorporating a 13-stage axial-flow compressor with a pressure ratio of approximately 7, rated engine speed of 8300 rpm, and air flow of approximately 120 pounds per second. The engine, which was installed and operated in a Lewis sea-level static test stand, was equipped with an adjustable exhaust nozzle to permit variation of the pressure ratio or air flow at a constant speed.

Methods of detecting and measuring vibratory stress. - Commercial resistance-wire strain gages were cemented to eight blades in each of the first three compressor stages at approximately midchord position as close as possible to the base of the airfoil section. The eight blades per stage were divided into two groups of four blades approximately 180° apart. Lead wires were run from the strain gages to a 19-ring slip-ring assembly mounted on the front of the engine starter. The slip-ring assembly and strain-gage circuits were the same as reported in reference 3.

A 12-channel recording oscillograph was used to record the strain-gage and hot-wire anemometer signals.

Hot-wire anemometer. - A constant-current hot-wire anemometer system was used to detect rotating stall. A 0.001-inch-diameter by 0.01-inch-length wire kept at a constant average temperature was used in each anemometer. The flow fluctuations were detected from the instantaneous variations in wire temperature. A resistance-capacitor-type compensator was used to obtain the necessary speed of response. Anamometer probes were installed in radial-survey devices located in the first, second, and third stator passages.

The hot-wire anemometer signals were viewed on a dual-beam cathode-ray oscilloscope, and permanently recorded on the 12-chanel recording oscillograph. The method used to determine the number of stall zones in a rotating-stall pattern was the same as used in references 1 and 4.

Pressure and temperature instrumentation. - The engine pressure and temperature instrumentation is shown in figure 1. Radial pressure and temperature rakes were installed ahead of the compressor inlet guide

vanes, compressor outlet, and the exhaust tail pipe. The air-flow measurements were calculated from the pressure and temperature measurements at station 1. All probes were spaced at area centers of equal annular areas.

PROCEDURE

The investigation was conducted in a sea-level static test stand with the compressor inlet and turbine exhaust open to the atmosphere. The engine was operated over a range of speeds from approximately 4500 to 8300 rpm with the adjustable exhaust nozzle set at various positions. The minimum nozzle area used was limited by maximum allowable tail-pipe temperature (1166° F), or the minimum area obtainable with the adjustable nozzle. At each condition, data were obtained to determine the compressor performance, and rotating-stall and rotor-blade-vibration characteristics.

RESULTS AND DISCUSSION

The data obtained in this investigation are discussed in their relation to the compressor performance and the effect of rotating stall on the rotor-blade vibration. The compressor used in this investigation was of the same production model as reported in reference 2.

Rotating-Stall Characteristics

The performance of the 13-stage compressor used in this investigation is presented in figure 2 as total-pressure ratio and adiabatic temperature-rise efficiency plotted against equivalent air flow. The data points along the solid line of figure 2(a) were taken with the exhaust nozzle set to give the approximate rated tail-pipe temperature at rated equivalent speed (8300 rpm). The data points along the lower line were taken with open exhaust nozzle or set to give maximum available area, and the data points taken along the upper line were taken with an exhaust area reduced from rated area.

The shaded section in figure 2(a) represents that area of operation where rotating stall was encountered, and hence, the unshaded section represents that area of operation where the compressor was free of rotating stall. Examination of the rated operational line indicates that there was no "marked" change in performance as the compressor became free of rotating stall. In the performance data in figure 2 of reference 2, a line was drawn indicating the operational limits of limiting turbine temperature, stall or surge, and at the lower speeds, minimum available exhaust area. As the result of a failure of a fourth-stage

rotor blade during this investigation, data were not obtained to draw this limiting type of line on the performance map of figure 2(a).

Figure 3(a) is a plot of vibratory stress against actual engine speed and percent of equivalent rated engine speed. A vibrating blade is affected by the actual speed; therefore, the vibration data will be discussed in terms of actual speed. The percent of equivalent rated speed can be used to locate the rotating-stall data on the performance curve in figure 2(a). Complete compressor data were not obtained for these data points. The data for this figure were obtained with the compressor operating with reduced nozzle area. At the bottom of the curve in figure 3(a) is a bar graph presenting the detailed rotating-stall data. As the compressor speed was increased, the stall-zone sequence was 5, 4, 3, 6, 5, and 4. The three-zone stall was the strongest and persisted over the longest speed range. At approximately 6240 rpm (74.5 percent of rated equivalent speed) the compressor was free of rotating stall.

Figure 3(b) is a plot of vibratory stress against actual speed and percent of equivalent rated engine speed. These data were obtained with the compressor operating on the open-nozzle line of figure 2(a). At the bottom of the curve is a bar graph presenting the detailed rotating-stall data. As the speed was increased, the stall zone sequence was 4, 3, and 5. As in figure 3(a), the three-zone pattern was the strongest and persisted over the longest speed range. At approximately 5870 rpm (70 percent of equivalent rated speed) the compressor was free of rotating stall. The operations of the jet engine with the reduced nozzle area or the compressor closer to the stall line increased the severity of the stall, the rotating-stall speed range, and the number of patterns. The six-zone pattern was observed only while operating with the minimum exhaust area.

Rotor-Blade Vibration

Figure 4 is a plot of frequency aganist "actual" engine speed. The dashed lines represent the natural bending frequencies for the first- to fourth-rotor stages corrected for the effect of centrifugal force (ref. 5). The lower series of data points represents the relative stall frequencies for the three-, four-, five-, and six-zone rotating stall over the range of speeds observed. The frequency of excitation due to rotating stall for a rotor blade is the stall frequency relative to the rotor blades. The relative stall frequency is defined by the following equation:

$$f_s' = \frac{N\lambda}{60} - f_s$$

where

f'_s relative stall frequency

N compressor speed

λ number of zones in a stall pattern

f_s absolute frequency determined from hot-wire signals

The upper series of data points represents the actual measured blade vibration frequencies for the first three stages. Over most of the speed range, the blade frequencies followed the dashed lines representing the static frequency corrected for the effect of centrifugal force. However, over the speed range of from approximately 4700 to 5700 rpm, the first-stage blades followed a line "B" representing a frequency equal to twice the relative stall frequency for the three-zone stall. Over a speed range of from 5300 to 6000 rpm, the second-stage blades also followed this two times three-stall line. These first- and second-stage blades were being forced to vibrate by the three-zone rotating stall. In reference 2, the first- and second-stage blades were also forced to vibrate at twice the relative frequency of the three-zone rotating stall and not their own natural frequencies. However, an exception did occur at approximately 5540 rpm (fig. 4). At this point the first- and second-stage blades were forced to vibrate at the frequency of a six-zone rotating stall. Shown in figure 3(a) are the stress data for the first three stages as the compressor was operating on the reduced-nozzle line in figure 2(a). The first stage had peak stress values of ±19,000 and ±31,200 pounds per square inch at approximately 5050 and 5540 rpm, respectively. The first peak stress was observed with a three-zone stall and the second peak with a six-zone stall. The stresses observed in the second stage were considerably lower than for the first stage. The average stress of the many peaks between 4800 and 6000 rpm was approximately ±12,000 pounds per square inch. The three- and five-zone stalls were observed with these vibrations. No stresses over ±6000 pounds per square inch were observed in the third stage.

In figure 3(b), with the compressor operating on the open-nozzle line, the first stage again had a peak stress at approximately 5000 rpm appearing with a three-zone stall. No peak stresses were observed at 5500 rpm because the six-zone stall was not present.

An examination of figures 3 and 4 indicates that the peak stresses existing at approximately 5000 rpm occurred at the point of intersection of the blade frequency line, and the line representing twice the relative frequency of the three-zone rotating stall. The peak stress of ±31,200 pounds per square inch (fig. 3(a)) was excited by a six-zone rotating-stall pattern. This stall pattern was observed over an extremely short speed range.

Figure 5 is a reproduction of sections of two oscillograph records. Section A is the record of the blade vibration occurring with a three-zone pattern at 5500 rpm. Here the first-stage blades were vibrating at a low maximum stress of ±7284 pounds per square inch. At this compressor speed, the three-zone stall had little effect on the blades, because the reltaive stall frequency was approximately 15 cycles higher than the natural blade frequency. Section B is a reproduction of the oscillograph record showing the maximum stress recorded in the first stage in this investigation. The compressor speed was 39 rpm higher than that for section A. However, in section B the compressor was operating with six-zone rotating stall. The rotational speed of the six-zone stall was higher than the three-zone stall and, as a result, the relative stall frequency for the six-zone stall was approximately 18 cycles lower than for the two times three stall (fig. 4). This reduction made the relative stall frequency equal to the natural blade frequency. With this fundamental excitation, the exciting forces were high and, as a result, the maximum vibratory stresses were observed.

Fourth-Stage Rotor-Blade Failure

After approximately 30 hours of engine operation at various speeds, the compressor case was removed to install additional instrumentation. As the case was removed, it was noticed that about 60 percent of a fourth-stage aluminum rotor blade was missing. The blade section was found wedged in the eleventh-stage stators. Figure 6(a) is a photograph of the failed blade and figure 6(b), a photograph of the fracture surface. An examination of this surface indicated that a fatigue failure had occurred.

Line A representing a frequency four times the relative stall frequency of a three-zone stall (fig. 4) intersects the fourth-stage blade frequency at approximately 4950 rpm. At this intersection, resonance would occur between the blades and rotating stall. Since strain gages had not been installed on the fourth stage, no blade vibration was recorded; however, it can be assumed that the fourth-stage blades would respond to the three-zone rotating-stall excitation as did the first and second stages (fig. 3).

SUMMARY OF RESULTS

A rotor-blade vibration and rotating-stall survey was conducted on a production 13-stage axial-flow compressor to determine the rotor-blade vibration and rotating-stall characteristics of a compressor with production changes. Strain gages and hot-wire anemometers were used to detect the blade vibrations and rotating stall, respectively. The results may be summarized as follows:

1. A maximum vibratory stress of ±31,200 pounds per square inch was measured in the first stage at approximately 5540 rpm. This vibration was a fundamental excitation by a six-zone rotating stall.

2. A three-zone stall pattern was the predominate stall pattern observed.

3. Stall patterns with three, four, five, and six zones were observed.

3561

4. The investigation was ended by a fourth-stage aluminum rotor-blade failure due to blade vibration excited by a three-zone stall pattern.

Lewis Flight Propulsion Laboratory
National Advisory Committee for Aeronautics
Cleveland, Ohio, December 2, 1954

REFERENCES

1. Huppert, Merle C., Calvert, Howard F., and Meyer, André J., Jr.: Experimental Investigation of Rotating Stall and Blade Vibration in the Axial-Flow Compressor of a Turbojet Engine. NACA RM E54A08, 1954.

2. Calvert, Howard F., Braithwaite, Willis M., and Medeiros, Arthur A.: Rotating-Stall and Rotor-Blade-Vibration Survey of a 13-Stage Axial-Flow Compressor in a Turbojet Engine. NACA RM E54J18, 1955.

3. Meyer, André J., Jr., and Calvert, Howard F.: Vibration Survey of Blades in 10-Stage Axial-Flow Compressor. II - Dynamic Investigation. NACA RM E8J22a, 1949. (Supersedes NACA RM E7D09.)

4. Huppert, Merle C.: Preliminary Investigation of Flow Fluctuations During Surge and Blade Row Stall in Axial-Flow Compressor. NACA RM E52E28, 1952.

5. Timoshenko, Stephen: Vibration Problems in Engineering. Second ed., D. Van Nostrand Co., Inc., 1937, p. 386.

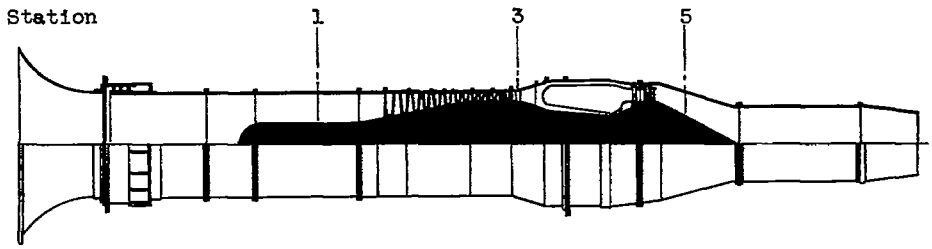

(a) Cross section of engine.

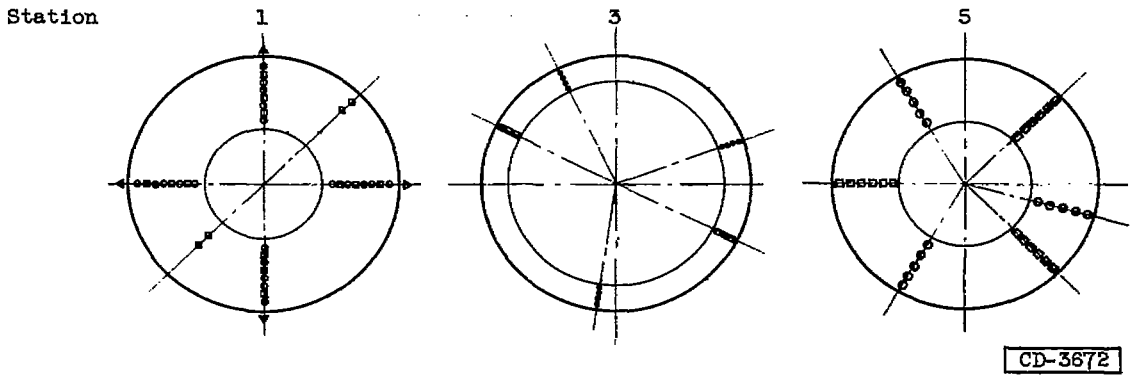

(b) Views of several stations (looking downstream).

Symbol	Type of probe	Station		
		1	3	5
○	Total pressure	20	12	15
□	Total temperature	12	6	18
△	Wall static tap	4	-	-
◇	Stream static	4	-	-

Figure 1. - Cross section of engine showing stations at which instrumentation was installed.

[redacted]

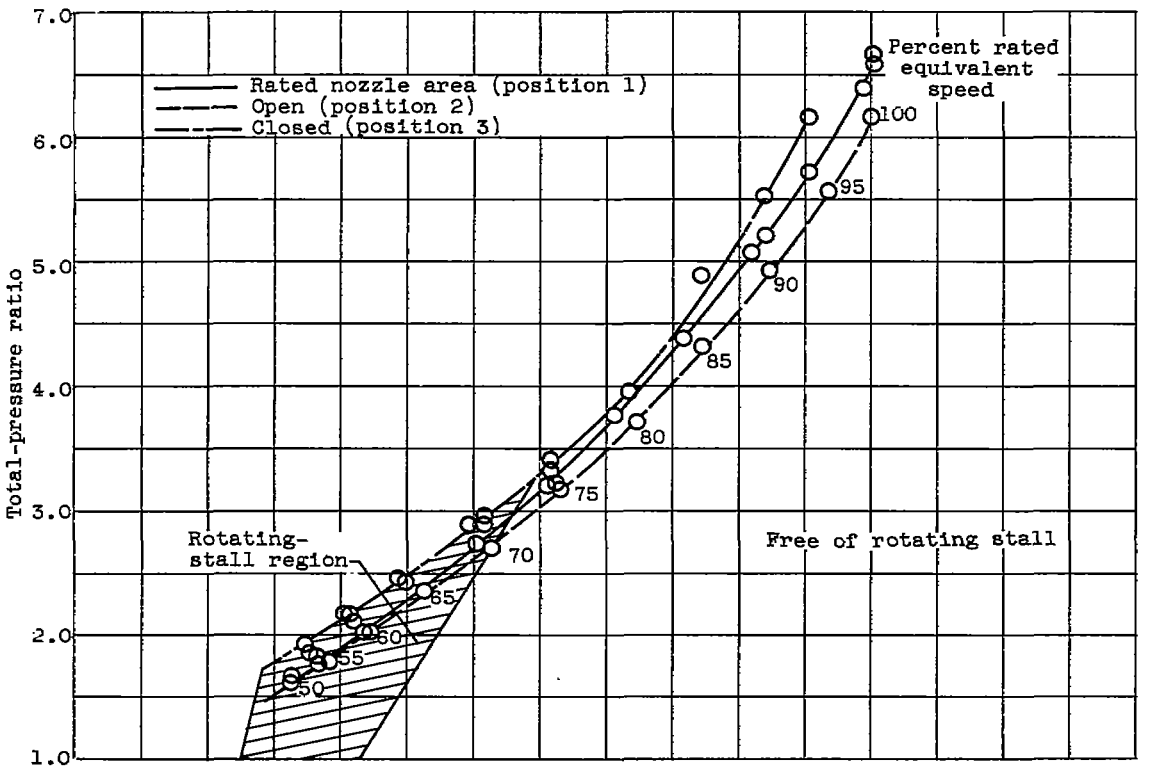

(a) Total-pressure ratio.

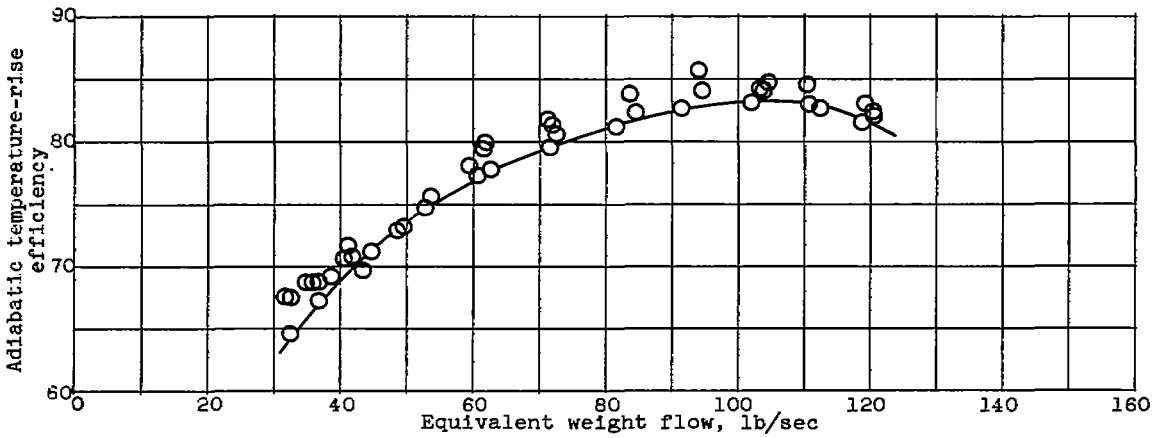

(b) Adiabatic temperature-rise efficiency.

Figure 2. - Compressor over-all performance.

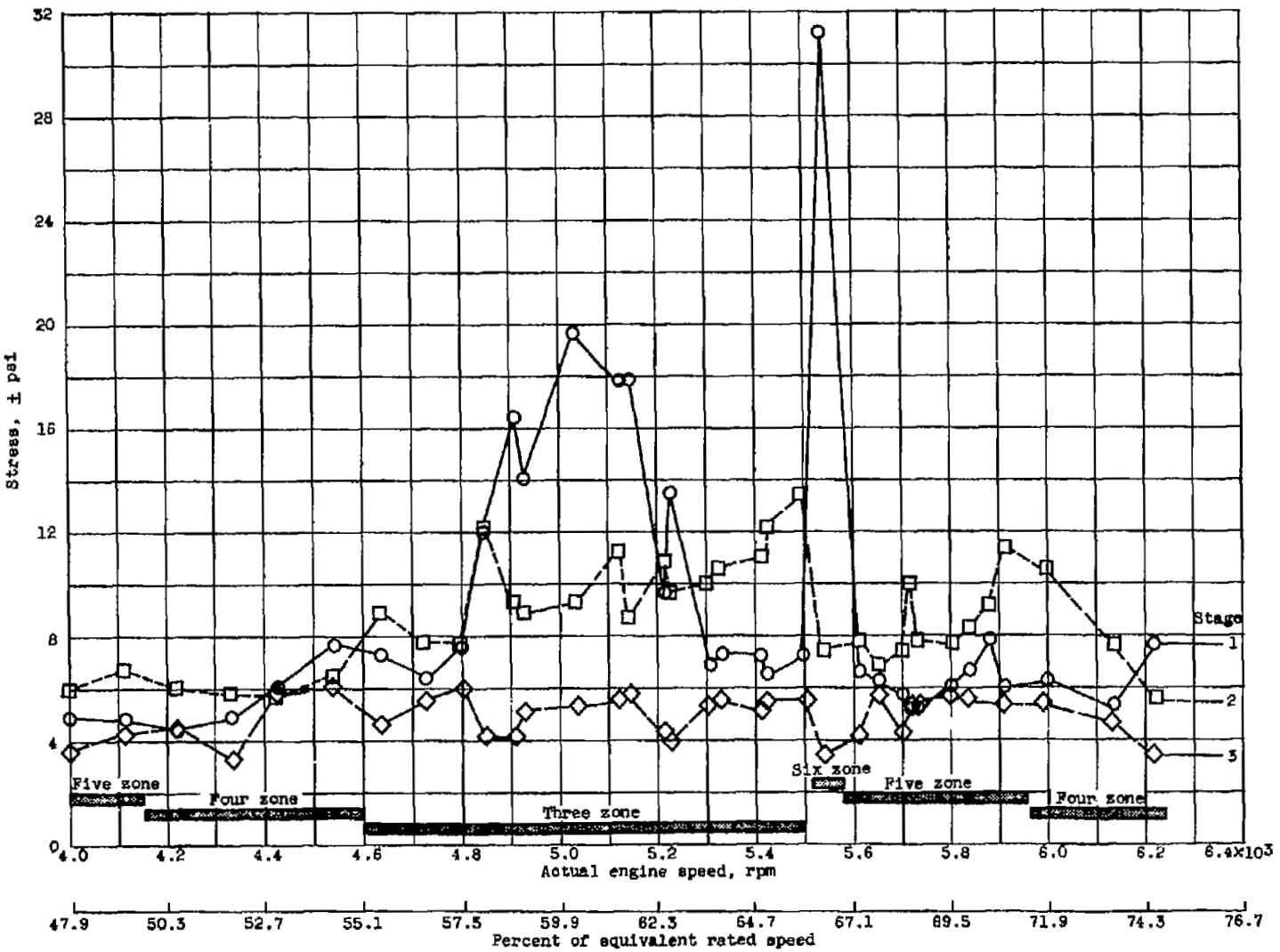

(a) Closed exhaust nozzle.

Figure 3. - Vibratory stresses and rotating-stall patterns measured in first three stages.

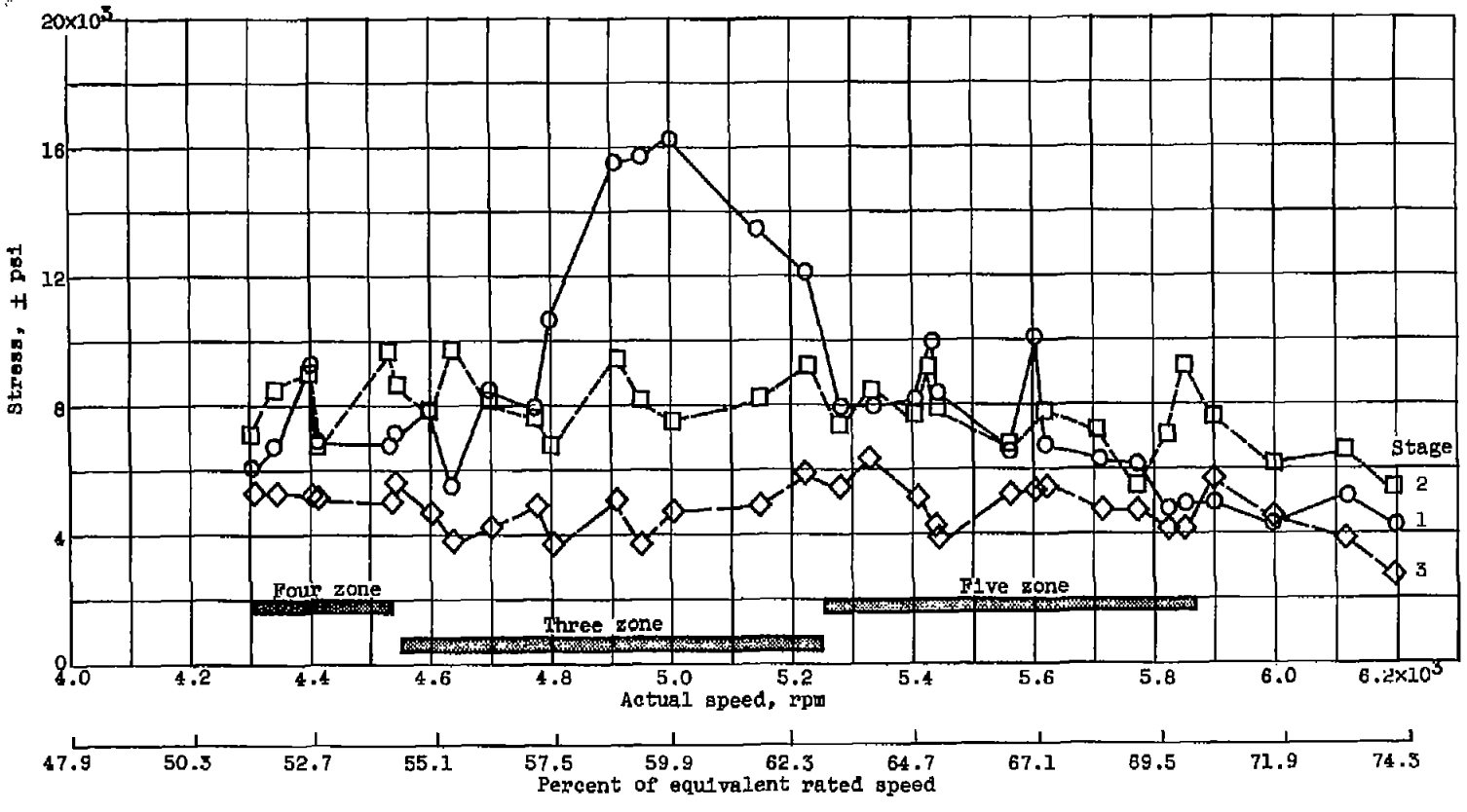

(b) Open exhaust nozzle.

Figure 3. - Concluded. Vibratory stresses and rotating-stall patterns measured in first three stages.

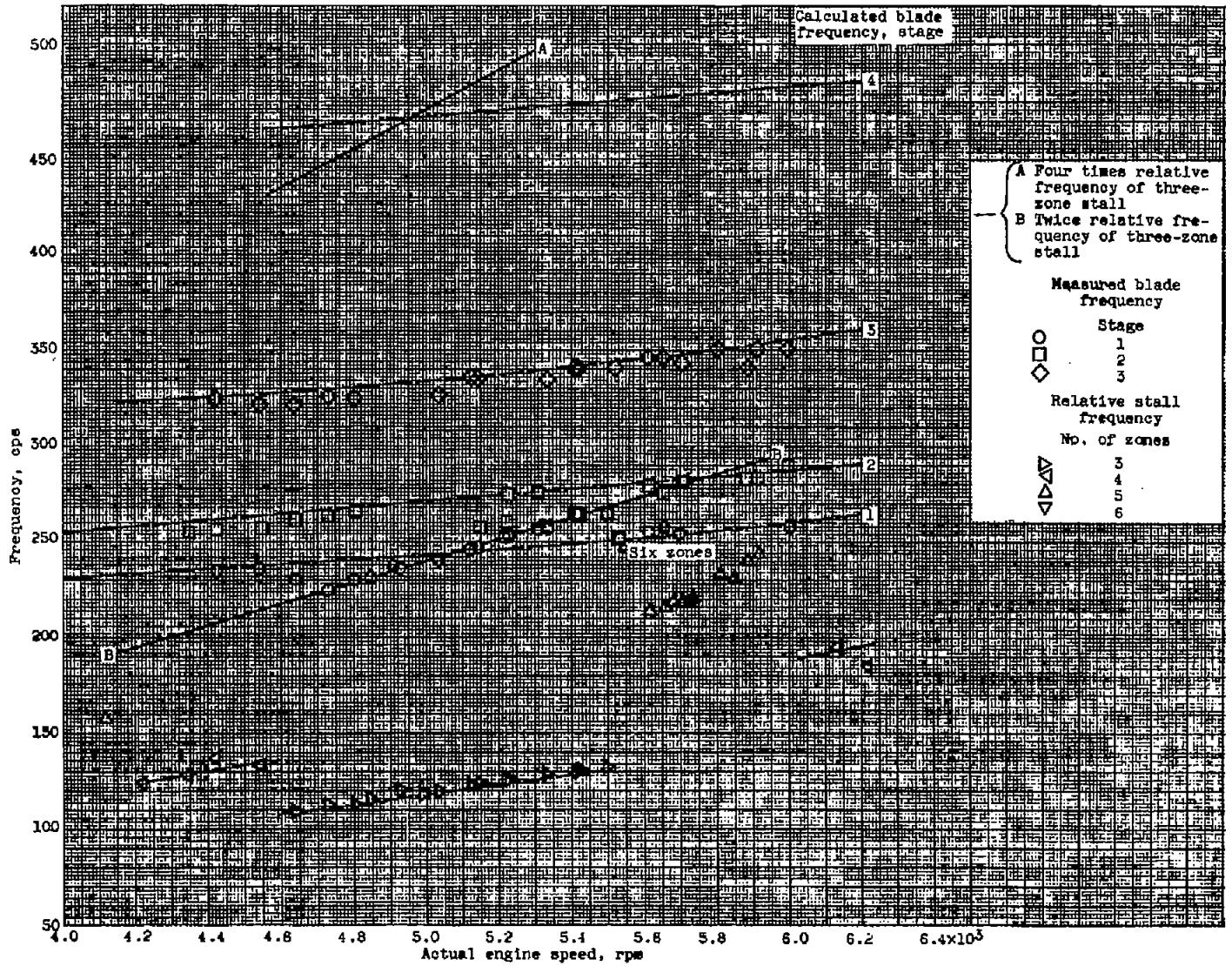

Figure 4. - Rotor-blade and rotating-stall frequencies for 13-stage axial-flow compressor.

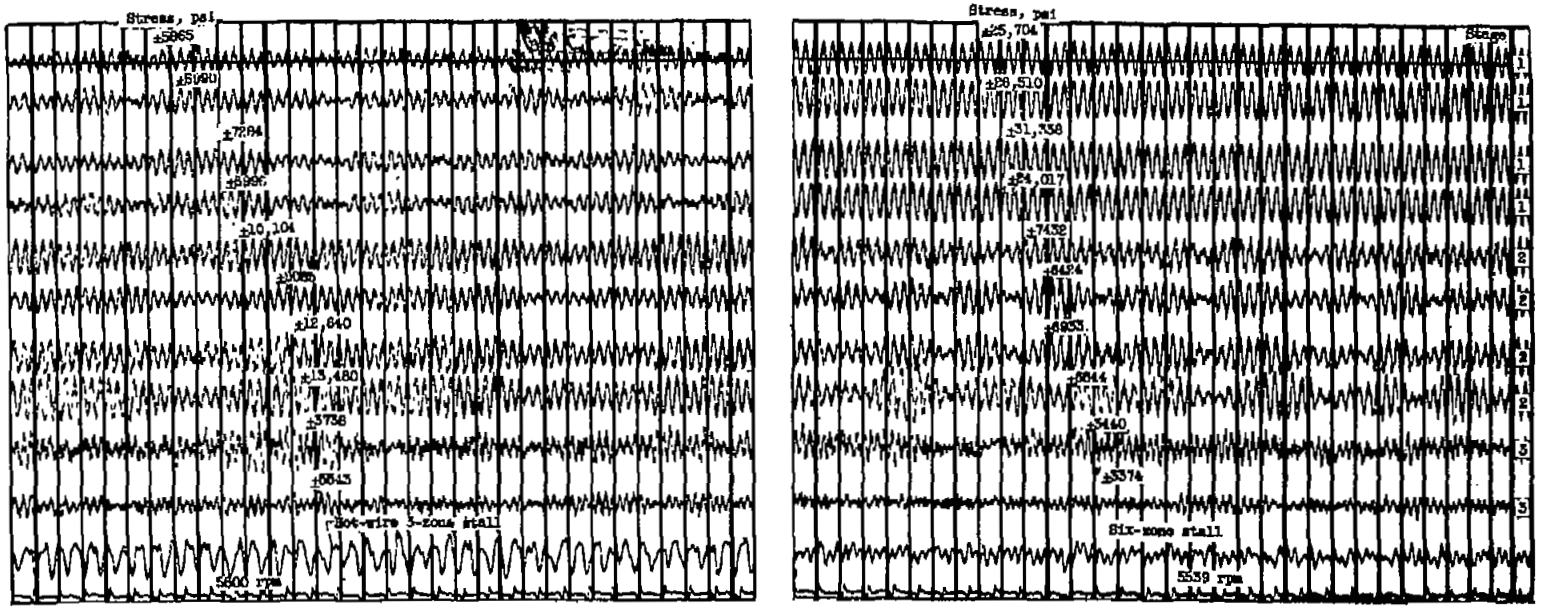

(a) Three-zone stall pattern.

(b) Six-zone stall pattern.

Figure 5. - Oscillograms of vibration caused by rotating stall.

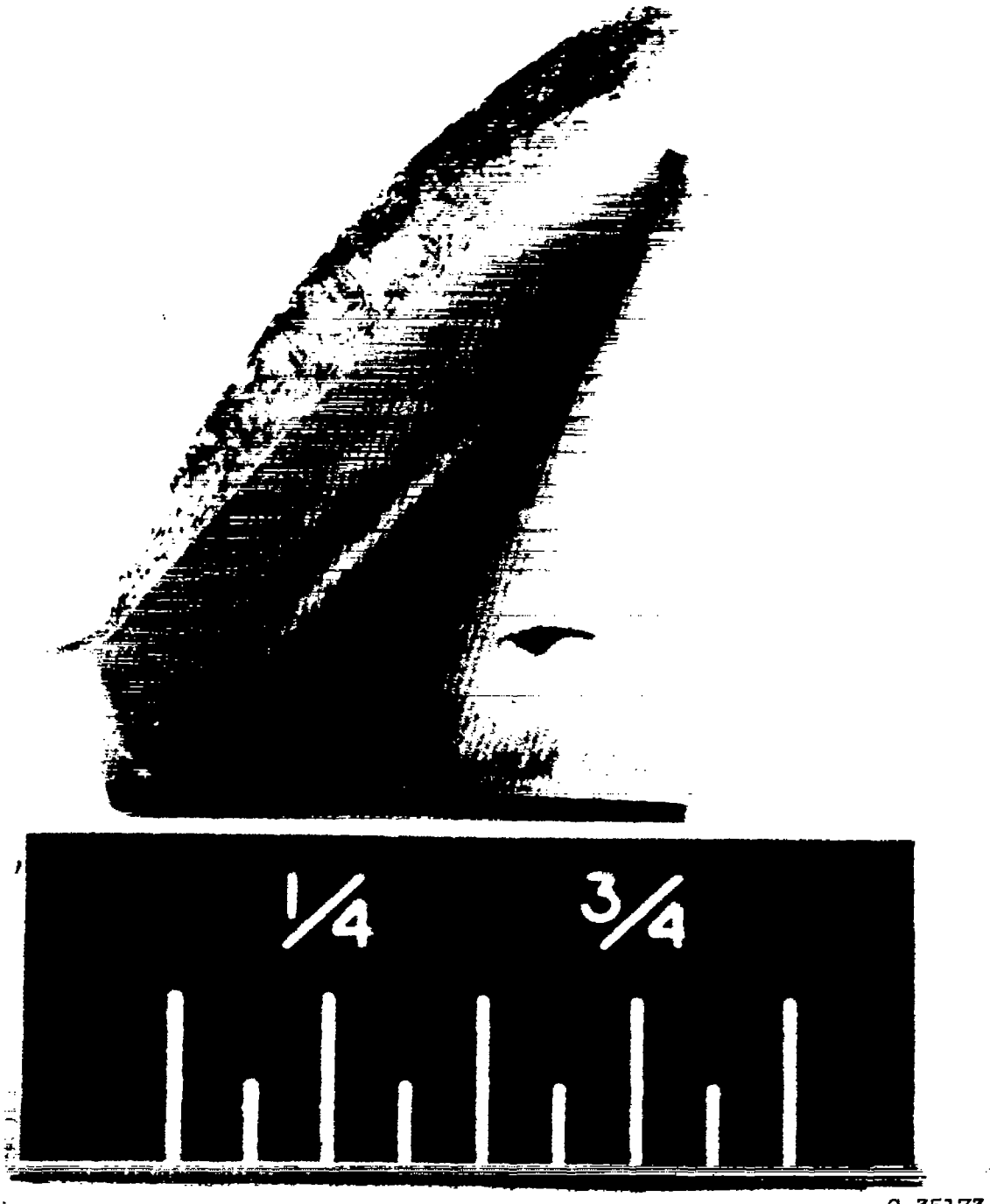

(a) Over-all view.

Figure 6. - Failed fourth-stage blade.

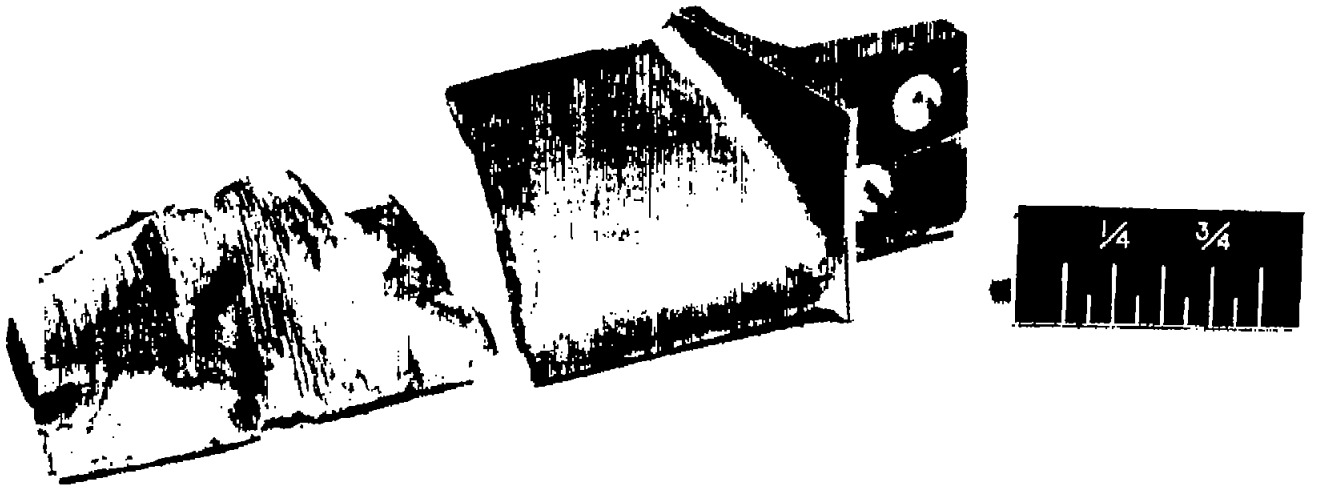

C-35174

(b) Fracture surface.

Figure 6. - Concluded. Failed fourth-stage blade.